



Copper isotopic composition of the silicate Earth



Sheng-Ao Liu^{a,*}, Jian Huang^b, Jingao Liu^c, Gerhard Wörner^d, Wei Yang^e, Yan-Jie Tang^e, Yi Chen^e, Limei Tang^f, Jianping Zheng^g, Shuguang Li^{a,b}

^a State Key Laboratory of Geological Processes and Mineral Resources, China University of Geosciences, Beijing 100083, China

^b CAS Key Laboratory of Crust–Mantle Materials and Environments, University of Science and Technology of China, Hefei, Anhui 230026, China

^c Department of Earth and Atmospheric Sciences, University of Alberta, 1-26 Earth Sciences Building, Edmonton, Alberta T6G 2E3, Canada

^d Geowissenschaftliches Zentrum Göttingen, Abt. Geochemie, Goldschmidtstr. 1, 37077 Göttingen, Germany

^e State Key Laboratory of Lithospheric Evolution, Institute of Geology and Geophysics, Chinese Academy of Sciences, P.O. Box 9825, Beijing 10029, China

^f The Second Institute of Oceanography, SOA, China

^g State Key Laboratory of Geological Processes and Mineral Resources, School of Earth Sciences, China University of Geosciences, Wuhan 430074, China

ARTICLE INFO

Article history:

Received 3 February 2015

Received in revised form 27 June 2015

Accepted 29 June 2015

Available online xxxx

Editor: D. Vance

Keywords:

copper isotopes
isotope fractionation
peridotite
basalt
silicate Earth

ABSTRACT

Copper isotopes have been successfully applied to many fields in geochemistry, and in particular, as a strongly chalcophile element, the isotope systematics of Cu can be potentially applied as a proxy for crust–mantle and core–mantle differentiation processes. However, to date, the Cu isotopic composition of distinct silicate reservoirs in the Earth, as well as the behaviour of Cu isotopes during igneous processes and slab dehydration are not well constrained. To address these issues, here we report high-precision ($\pm 0.05\%$; 2SD) Cu isotope data for 132 terrestrial samples including 28 cratonic peridotites, 19 orogenic peridotites, 70 basalts (MORBs, OIBs, arc basalts and continental basalts) and 15 subduction-related andesites/dacites sourced worldwide. The peridotites are classified into metasomatized and non-metasomatized groups, based upon their rare earth element (REE) patterns and the presence or lack of minerals diagnostic of metasomatism (e.g., phlogopite). The metasomatized peridotites span a wide range of $\delta^{65}\text{Cu}$ values from -0.64 to $+1.82\%$, in sharp contrast to the non-metasomatized peridotites that exhibit a narrow range of $\delta^{65}\text{Cu}$ from -0.15 to $+0.18\%$ with an average of $+0.03 \pm 0.24\%$ (2SD). Comparison between these two groups of peridotites demonstrates that metasomatism significantly fractionates Cu isotopes with sulfide breakdown and precipitation potentially shifting Cu isotopes towards light and heavy values, respectively. MORBs and OIBs have homogeneous Cu isotopic compositions ($+0.09 \pm 0.13\%$; 2SD), which are indistinguishable from those of the non-metasomatized peridotites within uncertainty. This suggests that Cu isotope fractionation during mantle partial melting is limited, even if sulfides are a residual phase. Compared with MORBs and OIBs, arc and continental basalts are more heterogeneous in Cu isotopic composition. In particular, basalts that were collected from a traverse across the Kamchatka arc over a distance of 200 to 400 km from the trench show a large range of $\delta^{65}\text{Cu}$ from -0.19 to $+0.47\%$, and samples with higher Ba/Nb ratios tend to be isotopically more heterogeneous. The large Cu isotopic variations in arc and continental basalts most probably reflect the involvement of recycling crustal materials in their sources.

Collectively, the dataset obtained in this study suggests that the bulk silicate Earth (BSE) has an average $\delta^{65}\text{Cu}$ value of $+0.06 \pm 0.20\%$ (2SD).

© 2015 Elsevier B.V. All rights reserved.

1. Introduction

Copper has two stable isotopes of ^{63}Cu and ^{65}Cu . As an important ore-forming metal, the stable isotopic systematics of Cu ($\delta^{65}\text{Cu}$ relative to NIST 976) has been widely applied as a tool for tracking

fluid pathways and fingerprinting sources of copper in porphyry systems (e.g., Mathur et al., 2009; Li et al., 2010). For example, Mathur et al. (2009) showed that different zones in porphyry copper deposits can be distinguished using Cu isotopes. Li et al. (2010) observed a systematic Cu isotopic variation from the core to outwards of the porphyry Cu–Au deposit at Northparkes, Australia and concluded that Cu isotopes can be applied to fingerprint hydrothermal processes. Apart from application to low-temperature

* Corresponding author.

E-mail address: lsa@cugb.edu.cn (S.-A. Liu).

fluid pathways, another important application of Cu isotopes is to trace the metal sources of copper deposits. Given that Cu in most porphyry deposits mainly originates from magmas, this application needs the knowledge of Cu isotopic compositions of silicate Earth reservoirs and possible Cu isotopic variations generated during magmatic processes.

On a more general level, as a strongly chalcophile element, Cu systematics in arc magmas has been used to constrain fluid enrichment and crust–mantle differentiation processes involved in the silicate Earth (Lee et al., 2012). The stable isotope system of Cu may hold the potential to constrain the crust–mantle differentiation and mantle–core differentiation processes that involve Cu partitioning between sulfides and silicates (Savage et al., 2015). For these applications the Cu isotopic compositions of the silicate Earth's reservoirs and possible Cu isotope fractionation during mantle partial melting, slab fluid enrichment and magmatic differentiation need to be constrained.

Li et al. (2009) showed that granitic rocks from SE Australia, representing the upper continental crust, generally have $\delta^{65}\text{Cu}$ values that cluster around zero, with average values of $+0.03 \pm 0.15\text{‰}$ for I-type granites and $-0.03 \pm 0.42\text{‰}$ for S-type granites. However, the copper isotopic composition of the upper mantle and thus the bulk silicate Earth (BSE) is not well constrained yet. To date, Cu isotope data have rarely been reported for mantle peridotites, with only two conference abstracts, which reported that $\delta^{65}\text{Cu}$ values of peridotites or ultramafic igneous rocks scatter around zero (Ben Othman et al., 2006; Savage et al., 2013). However, mantle peridotites are commonly subjected to metasomatism and therefore caution must be exercised when using them to estimate the BSE. In addition to peridotites, analyzing mantle-derived basalts is another approach to estimate the Cu isotopic composition of the BSE if partial melting does not produce isotopic effects for Cu. To date, there is also no systematic investigation on Cu isotopic compositions of various types of basalts (continental basalts, arc basalts, MORBs and OIBs). The limited data from international geostandards (BIR-1, BCR-2, BHVO-2, etc.) show that $\delta^{65}\text{Cu}$ values of basaltic rocks range from -0.01 to $+0.39\text{‰}$ (e.g., Archer and Vance, 2004; Bigalke et al., 2010; Moeller et al., 2012; Liu et al., 2014a, 2014b; Sossi et al., 2015).

During partial melting of the Earth's upper mantle, Cu behaves moderately incompatibly, as basaltic magmas show Cu concentrations three to five times their mantle source (Fellows and Canil, 2012). Because Cu in mantle rocks is mainly hosted in sulfides, it remains unclear whether or not Cu isotopes could be fractionated during partial melting of the mantle when sulfides are a residual phase. It has been shown that iron isotopes could be significantly fractionated during partial mantle melting (Weyer and Ionov, 2007). Therefore, whether or not Cu isotopes are fractionated during partial melting and whether the Cu-isotopic composition of basalts could represent their mantle source needs to be clarified.

To address these questions, we report a systematic study of Cu isotopes on (a) metasomatized and non-metasomatized peridotites from both cratonic regions and orogenic belts, (b) various types of basalts including mid-ocean ridge basalts (MORBs), oceanic island basalts (OIBs), arc basalts and continental basalts, and (c) subduction-related andesites and dacites from a variety of locations worldwide. The comprehensive dataset allows us to systematically investigate Cu isotope fractionation during mantle metasomatism and partial melting and to characterize Cu isotopic compositions of distinct silicate reservoirs in the Earth and, ultimately, the BSE on average.

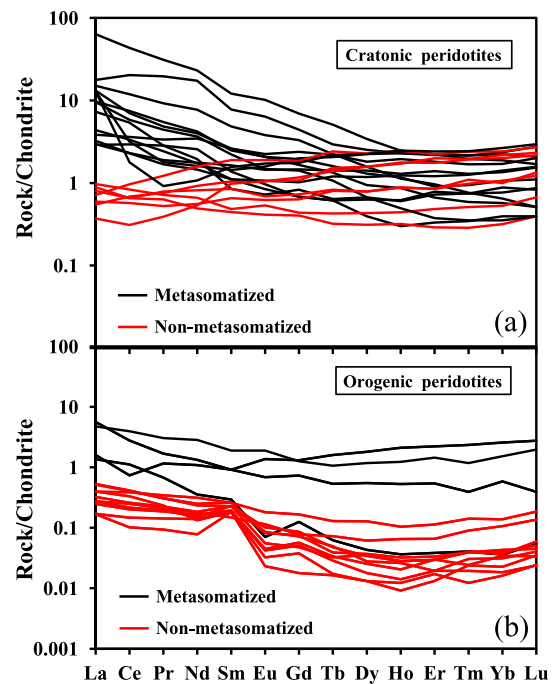


Fig. 1. The chondrite-normalized rare earth element (REE) patterns for cratonic peridotites (a) and orogenic peridotites (b) analyzed in this study. In each type, metasomatized and non-metasomatized peridotites are classified and plotted with different colors. The normalized values are after Sun and McDonough (1989).

2. Samples

2.1. Peridotites

The studied mantle peridotites include two types: cratonic and orogenic peridotites. The cratonic peridotites occur as xenoliths entrained by Cenozoic alkali basalts from three locations (Yangyuan, Fansi and Hannuoba) on the North China Craton (NCC). Petrography and chemical compositions of the xenoliths have been previously characterized (Rudnick et al., 2004; Liu et al., 2011). The samples comprise of spinel lherzolites, harzburgites and rare dunites, representing samples of the sub-continental lithospheric mantle. They span a wide range from typical refractory cratonic peridotites to fertile peridotites similar to the primitive upper mantle (Rudnick et al., 2004; Liu et al., 2011). The pattern of light rare earth elements (LREEs) is used here to evaluate the effect of metasomatism; those with $(\text{La}/\text{Sm})_N > 1$ are classified into metasomatized peridotites, where N represents chondrite normalization. Many of the studied cratonic peridotites have enriched LREEs and high $(\text{La}/\text{Sm})_N$, indicating significant metasomatism, whereas others have depleted LREEs and are not metasomatized (Fig. 1).

Orogenic peridotites are from two famous orogenic belts: the Alps and Dabie-Sulu. The Alpe Arami garnet peridotite from the Alpine collision zone (Switzerland) is composed of mainly olivine, two pyroxenes and up to 15% pyrope-rich garnet. This rock has an LREE-depleted pattern and represents a fragment of mantle rocks that was rapidly exhumed from mantle depths approaching or even exceeding 200 km (Olker et al., 2003). The Dabie-Sulu orogenic peridotites are from Raobazhai, Zhimafang and Xugou, including mainly dunite and harzburgite. All of these peridotites are mantle-derived and occur as blocks or lenses within exhumed gneiss (Zhang et al., 2000). Most of peridotites from Zhimafang and Xugou are phlogopite-bearing (Fig. S1) and have LREE-enriched patterns (Fig. 1), indicating that they have been metasomatized (Zheng et al., 2005, 2008), whereas those from Raobazhai are almost non-metasomatized.

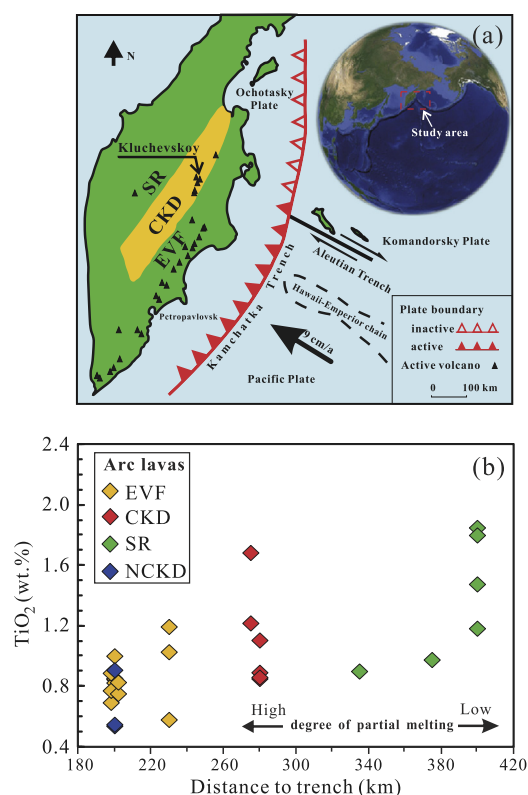


Fig. 2. (a) The geological map of the Kluchevskoy volcano in the Kamchatka arc, showing the location of Eastern Volcanic Front (EVF), Central Kamchatka Depression (CKD) and Sredinny Ridge (SR) with distance to trench, modified from Dorendorf et al. (2000). (b) Variation of TiO₂ contents of arc volcanic rocks with the distance to the trench. Data from Dorendorf et al. (2000) and Churikova et al. (2001).

2.2. Basalts

Basalts studied here comprise the four main types: MORBs, OIBs, arc basalts, and continental basalts. Six fresh MORBs are from the Carlsberg Ridge and the North Atlantic Ocean Ridge, located at 63°49.09'E, 3°42.06'N; 63°44.93'E, 3°40.20'N; 63°44.93'E, 3°40.20'N, respectively. Accreted Tertiary to Cretaceous OIBs are from the Azuero peninsula in south-central Panama (Buchs et al., 2011; Wegner et al., 2011), one of which is a strongly serpentinized cumulate rock. Back arc OIB-type alkaline basalts (<6 Ma) from north eastern Costa Rica (Abratis and Wörner, 2001) were also analyzed. Nine recently erupted OIB samples were from active hot spot volcanoes: transitional basalts to picrites from historic eruptions of Piton de la Fournaise volcano (Reunion) in the Indian Ocean, one sample from the 1974 tholeiitic Mauna Ulu eruption (Kilauea, Hawaii) in the central Pacific and one alkali basalt sample from the 1971 Teneguia eruption on the island of La Palma (eastern Atlantic Ocean).

Arc basalts are from the Kamchatka and Central America arcs. The Kamchatka basalts are from an arc traverse at 56°N, where active volcanoes are divided into three groups, including Eastern Volcanic Front (EVF), Central Kamchatka Depression (CKD) and Sredinny Ridge (SR) (Fig. 2a) (Dorendorf et al., 2000; Churikova et al., 2001). They display TiO₂ contents decreasing with increasing distance from the trench (Fig. 2b), indicating a change from higher degrees of partial melting near the arc front towards lower degrees and an enriched mantle component in the back arc (Churikova et al., 2001; Münker et al., 2004). The Kamchatka arc basalts are interpreted to have originated from a heterogeneous mantle, chemically affected by adding slab-derived fluids derived from the subducting Pacific crust (Churikova et al., 2001; Münker et al., 2004). Basalts from the Central American arc are from the arc and backarc

regions in southeastern Costa Rica (Abratis and Wörner, 2001) and Panama (Wegner et al., 2011).

Continental basalts are from four regions in the NCC (Tang et al., 2006; Yang and Li, 2008). These basalts share some common features with modern MORBs and OIBs and are interpreted to have been derived from the asthenospheric mantle. The basalts from Liaoxi were proposed to mainly have originated from the enriched lithospheric mantle metasomatized in the Early Cretaceous (Tang et al., 2006; Yang and Li, 2008). Enriched LREEs and LILEs suggest that the mantle source of some of these basalts had been metasomatized. A continental flood basalt from Antarctica was also analyzed for this study.

2.3. Andesites and dacites

Two high-Mg andesites are from Liaoxi in the NCC (Yang and Li, 2008). These rocks were proposed to have originated from partial melting of the enriched mantle with recycled crustal materials (Yang and Li, 2008). Eight andesites and one dacite are from the same E–W traverse in Kamchatka (see above) and from the Northern segment of the Central Kamchatka Depression (NCKD) at the junction at 57°N between the Kamchatka arc and the Komandorsky transform fault that links to the Aleutian arc (Churikova et al., 2001; Münker et al., 2004). The andesites from the EVF and SR have low Sr/Y and high Ba/Th ratios and are interpreted to contain a slab fluid component, while andesites from the NCKD have high Sr/Y and low Ba/Th ratios and are thought to contain a slab melt component (Yogodzinski et al., 2001). Two andesites and one dacite are from the Cordillera de Talamanca in the Central America arc (Abratis and Wörner, 2001).

3. Analytical methods

The detailed procedures for sample digestion, column chemistry and instrumental analysis in this study follow established methods (Liu et al., 2014a, 2014b; Li et al., 2015) modified from Maréchal et al. (1999). Only a brief description is given here.

At least 20 mg sample powders were weighed based on their known Cu concentrations and then digested in a mixture of double-distilled HF + HNO₃ + HCl in high-pressure bombs at 190 °C. The samples were transferred to beakers and dried down. After complete dissolution, 1 ml of 8 N HCl + 0.001% H₂O₂ was added to the beaker and evaporated to dryness at 80 °C. This process was repeated three times and the final material was dissolved in 1 ml of 8 N HCl + 0.001% H₂O₂ in preparation for ion-exchange separation. The dissolved solution was loaded through a column containing pre-cleaned AG-MP-1M resin, following the procedure outlined in Liu et al. (2014a) to separate Cu from the matrix. Because high Fe/Cu ratios of peridotites (up to ~10,000) may cause overloading and result in earlier occurrence of Cu, two or three separate Cu fractions collected from the same peridotites were merged to yield a new solution. The new solution was then subjected to a second column. The total procedural blank was 2 ng, which is typically less than 0.5% of loaded Cu (>0.4 μg) in the studied samples and thus considered negligible. The Cu fractions were evaporated to dryness, dissolved in 3% HNO₃, and then re-evaporated to dryness and re-dissolved in 3% HNO₃ to remove all chlorine prior to isotope analysis. Matrices Ti, Na, Mg and Fe were checked for each eluted Cu fraction and their ratios to Cu were found to be less than 0.1% for all samples, so these matrices led to insignificant influence on the accuracy of Cu isotope analysis (Liu et al., 2014a).

Copper isotopic ratios were measured using the Thermo Scientific Neptune plus MC-ICP-MS instruments at the Isotope Geochemistry Laboratory of the China University of Geosciences, Beijing.

Table 1

A summary of the weighted average value and range of copper isotopic compositions of peridotites, different types of basalts, andesites/dacites and geostandards reported in this study. The original data are reported in the Supplementary materials.

Rock type/name	$\delta^{65}\text{Cu}$ range (‰)	$\delta^{65}\text{Cu}$ average (‰)	2SD	N
Cratonic peridotites (metasomatized)	−0.64 to +0.68	0.11	0.52	23
Cratonic peridotites (non-metasomatized)	−0.15 to +0.18	0.03	0.26	7
Orogenic peridotites (metasomatized)	−0.34 to +1.82	0.02	0.60	10
Orogenic peridotites (non-metasomatized)	−0.19 to +0.28	0.03	0.21	9
MORBs	+0.04 to +0.14	0.09	0.08	6
OIBs	−0.07 to +0.18	0.09	0.14	14
Continental basalts	−0.18 to +0.35	0.10	0.24	27
Arc basalts	−0.19 to +0.47	0.16	0.21	23
All basalts	−0.19 to +0.47	0.11	0.21	70
Andesites/dacites	+0.04 to +0.38	0.12	0.30	15
Reference materials				
JP-1		0.03	0.05	3
BHVO-2		0.13	0.03	2
BCR-2		0.21	0.04	2
Repeat		0.19	0.03	3
BIR-1a		0.02	0.04	3
AGV-2		0.06	0.04	1

Sample-standard bracketing method was used to correct for instrumental mass fractionation and drifting. The measurements were performed using wet plasma at low-resolution mode. A 100 ppb Cu solution was sufficient to achieve 5–6 V signal on ^{63}Cu using the high-sensitivity (X) cones. For each measurement, data were collected over three blocks of 40 cycles with ~ 8 s integration. Copper isotope data are reported in standard δ -notation in per mil relative to the standard reference material (SRM) NIST 976:

$$\delta^{65}\text{Cu} = \left(\frac{(^{65}\text{Cu}/^{63}\text{Cu})_{\text{sample}}}{(^{65}\text{Cu}/^{63}\text{Cu})_{\text{NIST 976}}} - 1 \right) \times 1000$$

The analytical precision of an in-house Cu standard solution (YS-Cu) over a period of two years (2012–July to 2014–July) is $\pm 0.03\%$ (2SD; $N = 69$) (Fig. S2). The long-term external reproducibility for $\delta^{65}\text{Cu}$ measurements is better than $\pm 0.05\%$ (2SD) obtained from repeated analyses of natural samples and synthetic solutions (Liu et al., 2014a). International rock standards (BHVO-2, BCR-2, BIR-1a, AGV-2) were analyzed during the course of this study, yielding values (Table 1) which agree well with those reported by previous studies (Li et al., 2009; Bigalke et al., 2010; Moeller et al., 2012; Liu et al., 2014a). The peridotite JP-1 analyzed in this study has a $\delta^{65}\text{Cu}$ value of $+0.03 \pm 0.05\%$.

4. Results

The analytical methods and data of major and trace elements of orogenic peridotites measured in this study are listed in Table S1. Copper isotopic compositions of all peridotites are reported in Table S2, together with selected major elements, S contents and f_{O_2} . The data for basalts, andesites and dacites are reported in Table S3, together with selected major elements. The range and average value of $\delta^{65}\text{Cu}$ for peridotites, basalts, andesites and dacites are summarized in Table 1. Peridotites analyzed in this study exhibit a large variation of $\delta^{65}\text{Cu}$ values from -0.64 to $+1.82\%$. $\delta^{65}\text{Cu}$ values of the cratonic peridotites range from -0.64 to $+0.68\%$ with a total variation of 1.32% . The orogenic peridotites from the Dabie-Sulu have $\delta^{65}\text{Cu}$ from -0.34 to $+0.51\%$, with a sample (RC-1J) having an extreme value of $+1.82 \pm 0.04\%$. The garnet peridotite from the Alps has a $\delta^{65}\text{Cu}$ value of $-0.10 \pm 0.05\%$.

The MORBs from the Carlsberg Ridge and the North Atlantic Ocean Ridge have $\delta^{65}\text{Cu}$ varying from $+0.05$ to $+0.11\%$ (aver-

age = $+0.08\%$) and from $+0.04$ to $+0.14\%$ (average = $+0.09\%$), respectively. The accreted OIBs from the Azuero have $\delta^{65}\text{Cu}$ varying from $+0.04$ to $+0.18\%$ (average = $+0.14\%$; $n = 5$) with no difference shown for the serpentinized cumulate. Other OIBs from the Indian Ocean, Pacific Ocean and the Atlantic Ocean have $\delta^{65}\text{Cu}$ varying from -0.07 to $+0.13\%$. The arc basalts from two different arcs in Kamchatka and Central America with various distances to the trench have $\delta^{65}\text{Cu}$ from -0.19 to $+0.47\%$, with an average of $+0.13 \pm 0.26\%$. Other arc basalts and dacites from Kamchatka have $\delta^{65}\text{Cu}$ ranging from $+0.03$ to $+0.28\%$. Continental basalts from the NCC have $\delta^{65}\text{Cu}$ from -0.18 to $+0.35\%$ with an average of $+0.10\% \pm 0.24\%$. Two andesites from Yixian have $\delta^{65}\text{Cu}$ values of $+0.01$ and $+0.05\%$, respectively. The andesites from the Kamchatka and the Central American arcs have $\delta^{65}\text{Cu}$ values ranging from $+0.19$ to $+0.28\%$. The dacites have $\delta^{65}\text{Cu}$ values of -0.14 to $+0.07\%$.

5. Discussion

In this section, we first discuss the behaviour of Cu isotopes during mantle metasomatism, mantle partial melting and slab dehydration in subduction zones. Following this, we estimate the average Cu isotopic composition of the bulk silicate Earth.

5.1. Cu isotope fractionation triggered by mantle metasomatism

Metasomatism is often observed in orogenic peridotites or xenoliths carried by basaltic lavas to the surface. The influence of metasomatism must be evaluated prior to estimating chemical or isotopic composition of the mantle using peridotites. In particular, Cu in mantle rocks is mainly hosted in sulfides which are susceptible to metasomatism via melt/fluid–rock interaction. In the cratonic peridotites studied, the positive correlation of Cu concentrations with S (Fig. S3) confirms that Cu in these peridotites is mainly hosted by sulfides. The studied cratonic peridotites and orogenic peridotites can be classified into two groups: metasomatized and non-metasomatized based on their REE patterns (Fig. 1) and the presence or absence of secondary minerals diagnostic of metasomatism (e.g., phlogopite; Fig. S1). Most of the cratonic peridotites and some of the orogenic peridotites have enriched LREEs and some are phlogopite-bearing, indicating that they were metasomatized to various extents (Liu et al., 2010; Zheng et al., 2005).

As plotted in Fig. 3, the metasomatized cratonic and orogenic peridotites have highly variable Cu concentrations and are isotopically much more heterogeneous than the non-metasomatized peridotites. Such a large range of Cu isotopic composition (-0.64 to $+1.82\%$) in the metasomatized peridotites is difficult to be explained by high-temperature equilibrium Cu isotope fractionation, e.g., mantle partial melting (see below). Most of the metasomatized peridotites also have very high $(\text{La}/\text{Sm})_N$, indicating that metasomatism most likely is the cause for the large isotopic variations. **Metasomatism in peridotites can potentially result in sulfide dissolution/breakdown or sulfide precipitation (e.g., Reisberg et al., 2005). Sulfide dissolution/breakdown, if involving redox reaction, released Cu which could be isotopically heavy (Fernandez and Borrok, 2009), leaving the metasomatized peridotites isotopically lighter than the primary non-metasomatized peridotites.** By contrast, precipitation of secondary minerals from fluids previously leaching Cu in sulfides may enrich the peridotites in heavy Cu isotopes, although an isotopic fractionation may occur depending on which secondary phase was precipitating. These two processes may result in contrasting Cu isotope fractionation, and are expected to have occurred in the metasomatized peridotites examined that have $\delta^{65}\text{Cu}$ varying from -0.64 to $+1.82\%$ (Fig. 3).

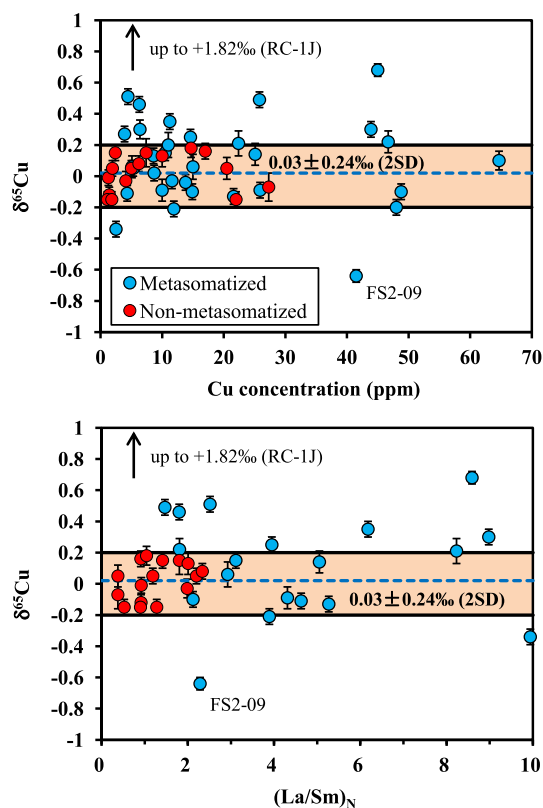


Fig. 3. Correlation of Cu isotopic compositions with Cu concentrations and $(\text{La}/\text{Sm})_N$ for peridotites reported in this study. The average $\delta^{65}\text{Cu}$ of all non-metasomatized peridotites is $+0.03 \pm 0.24\text{‰}$ (2SD; $N = 16$). Data are reported in Table S2.

5.2. Cu isotope fractionation during mantle melting

As a moderately incompatible element, Cu tends to be enriched in basaltic magmas relative to the mantle source. Primitive basaltic melts from mid-ocean ridges, ocean islands and arc settings generally contain three to five times more Cu than the primitive upper mantle (PUM) value, corresponding to a bulk partition coefficient D_{Cu} mantle/melt of ~ 0.20 – 0.30 (Fellows and Canil, 2012). For example, MORBs have an average Cu concentration of 90 ppm compared with the upper mantle of 29 ppm (Sun and McDonough, 1989). The measured sulfide/silicate melt partition coefficients (D_{Cu}) vary between 250 and 960, much larger than silicate minerals (ol, cpx, opx and grt)/melt D_{Cu} values (< 1.0) (Ripley et al., 2002; Lee et al., 2012). The degree of Cu enrichment in basaltic magmas is related to the presence of sulfide in mantle source, the melt/sulfide ratio, and the oxidation state of the mantle (Fellows and Canil, 2012; Lee et al., 2012). The possible effect of sulfides on Cu isotopes during mantle melting is evaluated below.

Mantle peridotites of different composition potentially underwent various degrees of melt extraction. Our data show a negative correlation of Al_2O_3 with MgO contents (Fig. S4), indicating various degrees of melt extraction. In particular, the non-metasomatized peridotites also exhibit negative correlation of Cu concentrations with MgO contents, which is not seen in the metasomatized peridotites due to the highly variable Cu concentrations (Fig. S4). The co-variation of Cu and MgO in the non-metasomatized peridotites most likely reflects melt extraction with Cu preferentially partitioning into the melts. On the other hand, different types of basalts may have been generated by different degrees of partial melting and different melting processes, e.g., OIBs are commonly generated by lower degrees of melting ($\sim 5\%$) (Mckenzie and O'Nions, 1995), MORBs by moderate melting (10–15%) (Klein and Karsten, 1995), and arc basalts by high degree of melting (10–25%) due to the

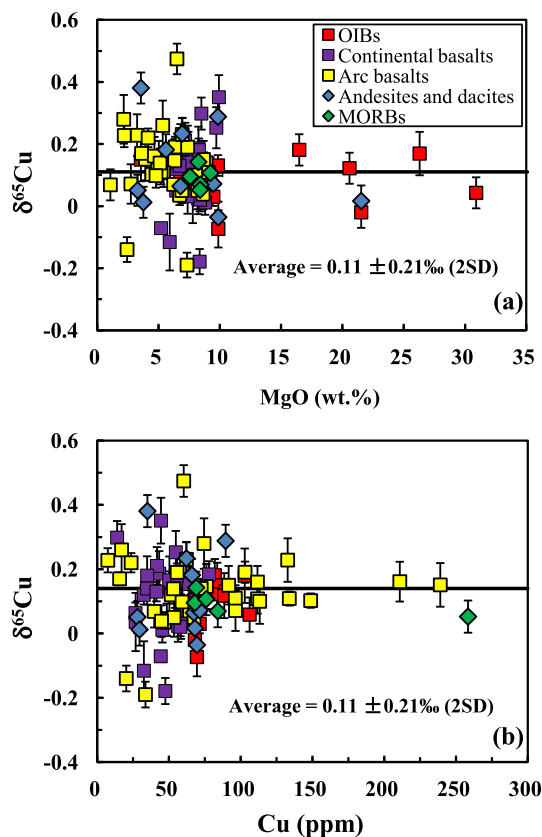


Fig. 4. Correlation of Cu isotopic ratios with MgO (a) and Cu (b) concentrations for basalts, andesites and dacites from worldwide. The average $\delta^{65}\text{Cu}$ of all basalts taken together is $+0.11 \pm 0.21\text{‰}$ (2SD; $N = 70$). Data are reported in Table S3.

addition of fluids released in subduction zones (Plank and Langmuir, 1998). Sulfide is predicted to be a residual phase until $\sim 25\%$ melting in a fertile mantle source (Hamlyn et al., 1985), hence the degree of melting normally associated with MORB and especially OIB will leave some Cu behind, potentially giving rise to isotope fractionation. In a conference abstract, Savage et al. (2014) showed that the isotopically lightest peridotite xenoliths ($\delta^{65}\text{Cu} = -0.40$ to -0.20‰) they analyzed are the most melt-depleted. They took this as strong evidence that mantle partial melting fractionates Cu isotopes.

Our approach is to directly compare the Cu isotopic compositions of the peridotites and their potential complementary derivatives – basalts. However, we see large Cu isotopic variations in arc basalts (-0.19 to $+0.47\text{‰}$) and continental basalts (-0.18 to $+0.35\text{‰}$), in sharp contrast to the relatively homogeneous Cu isotopic composition of MORBs ($+0.04$ to $+0.14\text{‰}$) and OIBs (-0.07 to $+0.18\text{‰}$). This observation (Figs. 4, 5) is in conflict with a simple melting mechanism that would shift the copper isotopic composition in one direction. For the continental basalts from the NCC, trace elements and Sr–Nd–Pb isotopes indicate that they have originated from the enriched lithospheric mantle with recycled crustal materials (Tang et al., 2006; Yang and Li, 2008). Therefore, their large Cu isotopic variation was most likely caused by the involvement of isotopically variable materials, e.g., by subduction-related addition or metasomatism by recycled crustal materials in the sub-continental mantle sources, as observed in the metasomatized peridotites from the NCC. For arc basalts, a similar explanation is proposed (see Section 5.3). When arc and continental basalts are excluded, the data show that the Cu isotopic compositions of MORBs and OIBs ($+0.09 \pm 0.13\text{‰}$; 2SD) are indistinguishable within uncertainty from those of the non-metasomatized peridotites ($+0.03 \pm 0.24\text{‰}$; 2SD). This suggests

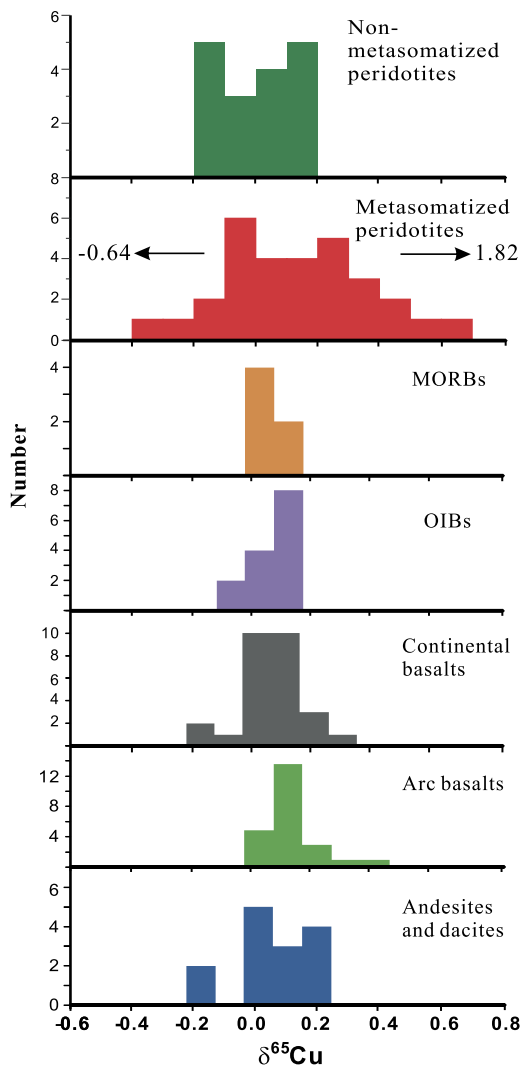


Fig. 5. Histograms of Cu isotopic compositions of metasomatized and non-metasomatized peridotites, various types of basalts and andesites/dacites reported in this study (Tables S2 and S3).

that mantle partial melting generates a limited Cu isotope fractionation, distinct from the conclusion as proposed by Savage et al. (2014) based on a study of peridotites.

The formal valence of Cu in silicate depends on the fugacities of oxygen and sulfur, as well as the presence of iron. High oxygen fugacity would transform Cu^+ to Cu^{2+} , whereas high sulfur fugacity could stabilize the sulfide phase which contains a formal valence of Cu^+ (e.g., Cu_2S) in these sulfide melts. At the range of oxygen fugacity (f_{O_2}) typical of most igneous rocks, the formal valence of Cu in silicate melts is close to unity (Ripley et al., 2002). At the f_{O_2} values of $\Delta\text{FMQ} = -1$ to 0 (log 10 unit deviations from the fayalite–magnetite–quartz buffer), typical of the average upper mantle, sulfides are stable with S^{2-} as the dominant valence state (Lee et al., 2012). In this case, sulfide containing monovalent Cu dominates mantle Cu, provided that Cu does not significantly partition into non-sulfide phases. Thus, the absence of significant change of the valence of Cu may account for the limited Cu isotope fractionation during partial melting of mantle rocks, even if sulfides are a residual phase. The absence of significant Cu isotope fractionation during mantle melting is in contrast to Fe isotopes which are significantly fractionated during mantle partial melting, with the melts enriched in heavy Fe isotopes by $\sim 0.1\%$ in $\delta^{56}\text{Fe}$ relative to the mantle source (Weyer and Ionov, 2007).

As discussed above, all basalts including MORBs, OIBs, arc basalts and continental basalts have statistically indistinguishable Cu isotopic composition on average (Figs. 4, 5) and no correlation is observed between $\delta^{65}\text{Cu}$ and MgO contents. Andesites and dacites also have variable Cu isotopic compositions similar to those of arc and continental basalts (Figs. 4, 5). Given the significant $\delta^{65}\text{Cu}$ range of arc and continental basalts, the Cu isotopic variations in andesites and dacites may reflect isotopic heterogeneity of their parent magmas. Savage et al. (2013) suggested that Cu isotopes can be fractionated towards heavy or light values, depending on the crystallizing phases. Alternatively, the $\delta^{65}\text{Cu}$ variations observed in andesites and dacites may be partially attributed to Cu isotope fractionation during magmatic differentiation (Savage et al., 2013). Future studies are needed to determine to what extents magmatic differentiation could fractionate Cu isotopes.

5.3. Cu isotope fractionation during dehydration in subduction zones

Copper is considered a highly fluid-mobile element during hydrothermal ocean crust alteration and slab dehydration in subduction zones. Experimental studies show that up to 60% of Cu in the subducted basaltic oceanic crust could be released during dehydration processes from amphibolite to eclogite facies (Kogiso et al., 1997). The mobility of Cu during slab subduction and dehydration has an important bearing on Cu transport from subduction zones into the mantle wedge. Arc magmas generated in the arc mantle wedge are the primary host of porphyry copper deposits, and thus evaluating the transport of Cu from subduction slabs to the arc mantle is crucial to understanding the generation of porphyry copper deposits. Recent studies have debated the mechanisms of Cu enrichment in copper porphyries, e.g., an anomalously copper-rich source in the subducting slab or arc mantle, due to sulfide breakdown at oxidized conditions (Mungall, 2002). Alternatively, copper enrichment enhanced by magmatic differentiation processes within the thickened crust of the upper plate, without significant contributions from the mantle or subducting slabs has been proposed (Lee et al., 2012), e.g., for the Central Andes (Chiaradia, 2014). Copper isotopes may be a potential tool to distinguish these two hypotheses if they are significantly fractionated during magmatic differentiation or slab dehydration. We test the feasibility via investigating the behaviour of Cu isotopes during magmatic differentiation and slab dehydration.

To investigate potential Cu isotope fractionation during slab dehydration, we examined basalts from the Central American and the Kamchatka arcs. Subduction-related basalts, andesites and dacites from various arc settings have Cu isotopic compositions similar to those of MORBs and OIBs (Fig. 5). A more detailed investigation into arc lavas from Kamchatka is designed to cover a large across-arc region and thus a range of subduction fluid signatures related to slab dehydration and hydrous melting, and of crystal-melt fractionation and magma mixing (Dorendorf et al., 2000). Only samples close to the trench have negative $\delta^{65}\text{Cu}$ values, and a sample far away from the trench has the heaviest $\delta^{65}\text{Cu}$ (Fig. 6). Two possible mechanisms may explain this observation: isotopic heterogeneity of the arc mantle source and slab fluids involved in melting or different degrees of partial melting.

As shown in Fig. 2, lower TiO_2 contents with distance close to the trench indicate higher degrees of partial melting due to early addition of H_2O from down-going slabs. Samples close to the trench have highly variable Cu concentrations and some of them display Cu enrichments compared to those far from the trench (Fig. 6). By contrast, several samples close to the trench exhibit Cu depletion which may be due to dilution by high degrees of partial melting, reconciling with a small difference of Cu concentrations between arc basalts (54 ± 9 to 99 ± 26 ppm), OIBs (80 ± 31 to 121 ± 26 ppm), and MORBs (81 ± 23 ppm) from worldwide oc-

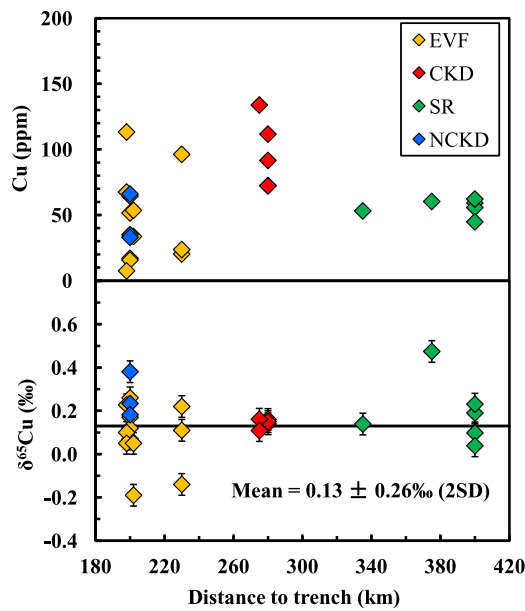


Fig. 6. The variation of Cu concentration and isotopic compositions of arc lavas as a function of the distance to the trench. The average $\delta^{65}\text{Cu}$ of all arc basalts taken together is $+0.13 \pm 0.26\text{‰}$ (2SD; $N = 25$). Data are reported in Table S3.

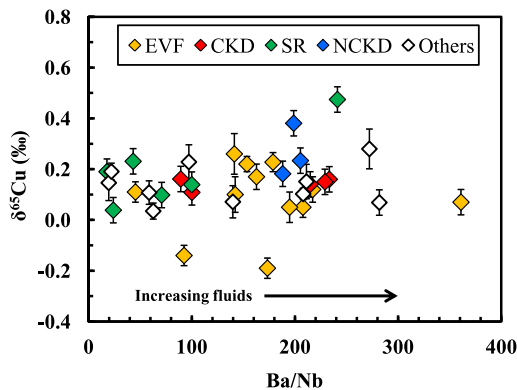


Fig. 7. The correlation of Cu isotopic compositions of arc lavas with Ba/Nb ratios. All Cu isotope data are from Table S3 and Ba and Nb concentrations are from previous studies (Dorendorf et al., 2000; Churikova et al., 2001; Münker et al., 2004). 'Others' denotes the studied samples for which no data of distance to the trench are available.

currences (Fellows and Canil, 2012 and reference therein). It is possible that the heavy $\delta^{65}\text{Cu}$ values far away from the trench compared with the light values close to the trench may result from lower degree of partial melting with distance to the trench. Nevertheless, the magnitude of Cu isotope fractionation during mantle partial melting as demonstrated above is too limited to explain the large variation in arc basalts (-0.19 to $+0.47\text{‰}$). Notably, arc samples with higher Ba/Nb ratios tend to show larger variations in Cu isotopic compositions (Fig. 7). This suggests that heterogeneity of the arc mantle sources caused by slab fluids is the most likely explanation for the large Cu isotopic variation observed in arc lavas.

5.4. Cu isotopic composition of the BSE and comparison with other reservoirs

It is generally suggested that igneous rocks have an average $\delta^{65}\text{Cu}$ close to zero. For example, Zhu et al. (2000) reported $\delta^{65}\text{Cu} \cong 0 \pm 0.5\text{‰}$ for chalcopyrites from igneous-hosted ore deposits. Li et al. (2009) reported average values of $+0.03 \pm 0.15\text{‰}$ for I-type granites and $-0.03 \pm 0.42\text{‰}$ for S-type granites from

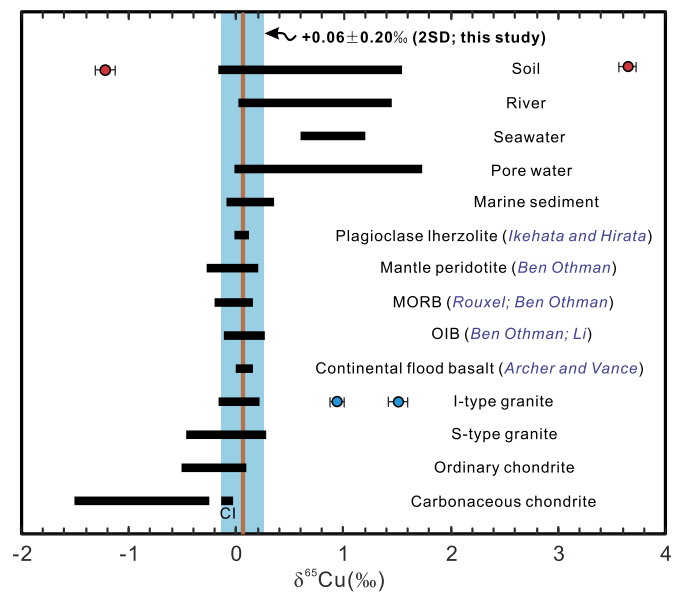


Fig. 8. The $\delta^{65}\text{Cu}$ ranges of peridotites, basalts and other geological reservoirs. The data of peridotites and basalts from previous studies are also shown for comparison. Data source: soil (Liu et al., 2014b, and reference therein), river (Vance et al., 2008), seawater (Vance et al., 2008), porewaters (Mathur et al., 2012), marine sediments (Maréchal et al., 1999), plagioclase lherzolites (Ikehata et al., 2011), mantle peridotites (Ben Othman et al., 2006), MORBs (Ben Othman et al., 2006), OIBs (Ben Othman et al., 2006; Li et al., 2009), continental flood basalts (USGS BCR-1) (Archer and Vance, 2004), I-type and S-type granites from the Lachlan fold belt, southeast Australia (Li et al., 2009), and carbonaceous chondrite and ordinary chondrite (Luck et al., 2003).

Australia. In a conference abstract, Savage et al. (2013) reported an average $\delta^{65}\text{Cu}_{\text{BSE}}$ value of $+0.07 \pm 0.12\text{‰}$ (2SD) based on komatiites, basalts and orogenic lherzolites. The comprehensive dataset obtained in this study allows us to accurately and precisely characterize the Cu isotopic composition of the BSE. The non-metasomatized peridotites have an average $\delta^{65}\text{Cu}$ of $+0.03 \pm 0.24\text{‰}$ (2SD), consistent with the value weighted by Cu concentrations ($+0.02 \pm 0.24\text{‰}$; 2SD). However, given the limited Cu isotope fractionation during mantle partial melting as demonstrated in this study, it is more reasonable to estimate Cu isotopic composition of the BSE based on the average value of non-metasomatized peridotites, MORBs and OIBs. This new estimate suggests that the BSE has an average $\delta^{65}\text{Cu}$ of $+0.06 \pm 0.20\text{‰}$ (2SD). The limited data from a previous abstract on mantle peridotites (Ben Othman et al., 2006) and a recent study on one San Carlos olivine (Sossi et al., 2015) generally fall within the range of the present study (Fig. 8).

Compared to the bulk silicate Earth, chondrites are more fractionated in Cu isotopic composition, and chondrites from most groups are enriched in ^{63}Cu , with $\delta^{65}\text{Cu}$ varying from -1.50 to -0.09‰ in carbonaceous chondrites and -0.51 to $+0.10\text{‰}$ in ordinary chondrites (Luck et al., 2003). The large Cu isotopic variations have been attributed to the mixing between two or more distinct isotopic reservoirs in the early solar system (Luck et al., 2003). A reasonable explanation for the Cu isotope discrepancy between the BSE and chondrites replies on Cu isotope fractionation during iron-sulfide/silicate segregation during core formation and core-mantle interaction. A recent study proposed that the heavier Cu isotopic composition of the BSE than the chondritic bulk Earth may result from preferential partitioning of light Cu isotopes into sulphide during core formation (Savage et al., 2015). This evokes the potential using Cu isotopes to understand the core-mantle differentiation process. Compared with the silicate reservoirs in the Earth, seawater, rivers and porewaters generally have heavy Cu isotopic compositions (Vance et al., 2008; Boyle et al., 2012). These isotopic variations reflect large Cu iso-

top fractionation during low-temperature redox transformation, indicating the potential applications of Cu isotopes as a powerful tracer in the field of low temperature mineralizing processes and environmental geochemistry.

6. Conclusion

We report a comprehensive copper isotope dataset ($n = 132$) for terrestrial samples including cratonic and orogenic peridotites, various types of basalts and dacites/andesites from worldwide occurrences. The aim of this study is to systematically investigate Cu isotope fractionation during mantle metasomatism and partial melting and to characterize Cu isotopic compositions of distinct silicate reservoirs in the Earth and, ultimately, the BSE on average.

Both metasomatized and non-metasomatized peridotites have been analyzed. Compared to the non-metasomatized peridotites, the metasomatized peridotites have highly variable Cu concentrations and isotopic compositions ($\delta^{65}\text{Cu}$ varying from -0.64 to $+1.82\%$). Sulfide dissolution-breakdown or mineral precipitation due to metasomatism potentially results in negative or positive effects of Cu isotopic ratios in peridotites as observed. Overall, the heavier average $\delta^{65}\text{Cu}$ value of the metasomatized peridotites in comparison with the non-metasomatized peridotites indicates that metasomatism seems to cause Cu isotopes towards heavier values on average.

MORBs and OIBs have homogeneous Cu isotopic compositions dramatically distinct for the large range observed in arc basalts and continental basalts. The heterogeneous Cu isotopic compositions of arc basalts and continental basalts may be due to the involvement of recycling crustal materials in the mantle sources. Arc lavas from the across-arc traverse in Kamchatka exhibit a large $\delta^{65}\text{Cu}$ range, which provides clear evidence that involvement of fluids from subducted slabs could cause significant Cu isotopic variation.

Copper isotopic compositions of MORBs and OIBs are not significantly different from those of the non-metasomatized peridotites, indicating a limited Cu isotope fractionation during mantle partial melting, even if sulfides are a residual phase in low degrees of partial melting (e.g., $<25\%$). Given that metasomatism appears to cause significant Cu isotope fractionation and Cu isotope fractionation during mantle partial melting is limited, the non-metasomatized peridotites, MORBs and OIBs are used to estimate a BSE. Accordingly, the new BSE estimate for $\delta^{65}\text{Cu}$ has a value of $+0.06 \pm 0.20\%$ (2SD).

Acknowledgements

We are grateful to Dr. Roberta Rudnick for sharing some of the peridotite samples analyzed in this study. The Alpe Arami sample was provided to GW by Gerhard Brey, Frankfurt, and sampling on Reunion Island was aided by N. Braumüller and A. diMuro. Three samples from Shiveluch volcano and Kamchatka were provided by T. Churikova. Dandan Li, Yiwen Lv and Ze-zhou Wang are thanked for their assistance in the lab. We thank R. Mathur and an anonymous reviewer for constructive comments and Editor Derek Vance for handling, which significantly improved the manuscript. This work is supported by the National Natural Foundation of China (41473017) to S.A.L., the National Key Basic Research Program of China (2015CB755905) to L.M.T., and the fundamental research funds (2-9-2014-068).

Appendix A. Supplementary material

Supplementary material related to this article can be found online at <http://dx.doi.org/10.1016/j.epsl.2015.06.061>.

References

- Abratis, M., Wörner, G., 2001. Ridge collision, slab-window formation, and the flux of Pacific asthenosphere into the Caribbean realm. *Geology* 29, 127–130.
- Archer, C., Vance, D., 2004. Mass discrimination correction in multiple-collector plasma source mass spectrometry: an example using Cu and Zn isotopes. *J. Anal. At. Spectrom.* 19, 656–665.
- Ben Othman, D., Luck, J.M., Bodinier, J.L., Arndt, N.T., Albarede, F., 2006. Cu–Zn isotope variation in the Earth's mantle. *Geochim. Cosmochim. Acta* 70 (18), A46.
- Bigalke, M., Weyer, S., Kobza, J., Wilcke, W., 2010. Stable Cu and Zn isotope ratios as tracers of sources and transport of Cu and Zn in contaminated soil. *Geochim. Cosmochim. Acta* 74, 6801–6813.
- Boyle, E.A., John, S., Abouchami, W., Adkins, J.F., Echegoyen-Sanz, Y., Ellwood, M., Flegal, A.R., Fornace, K., Gallon, C., Galer, S., 2012. GEOTRACES IC1 (BATS) contamination-prone trace element isotopes Cd, Fe, Pb, Zn, Cu, and Mo inter-calibration. *Limnol. Oceanogr., Methods* 10, 653–665.
- Buchs, D.M., Arculus, R.J., Baumgartner, P.O., Ulianov, A., 2011. Oceanic intraplate volcanoes exposed: example from seamounts accreted in Panama. *Geology* 39, 335–338.
- Chiaradia, M., 2014. Copper enrichment in arc magmas controlled by overriding plate thickness. *Nat. Geosci.* 7, 43–46.
- Churikova, T., Dorendorf, F., Wörner, G., 2001. Sources and fluids in the mantle wedge below Kamchatka, evidence from across-arc geochemical variation. *J. Petrol.* 42, 1567–1593.
- Dorendorf, F., Wiechert, U., Wörner, G., 2000. Hydrated sub-arc mantle: a source for the Kluchevskoy volcano, Kamchatka/Russia. *Earth Planet. Sci. Lett.* 175, 69–86.
- Fellows, S.A., Canil, D., 2012. Experimental study of the partitioning of Cu during partial melting of Earth's mantle. *Earth Planet. Sci. Lett.* 337–338, 133–143.
- Fernandez, A., Borrok, D.M., 2009. Fractionation of Cu, Fe, and Zn isotopes during the oxidative weathering of sulfide-rich rocks. *Chem. Geol.* 264, 1–12.
- Hamlyn, P.R., Keays, R.R., Cameron, W.E., Crawford, A.J., Waldron, H.M., 1985. Precious metals in magnesian low-Ti lavas: implications for metallogenesis and sulfur saturation in primary magmas. *Geochim. Cosmochim. Acta* 49, 1797–1811.
- Ikehata, K., Notsu, K., Hirata, T., 2011. Copper isotope characteristics of copper-rich minerals from Besshi-type volcanogenic massive sulfide deposits, Japan, determined using a femtosecond LA-MC-ICP-MS. *Econ. Geol.* 106, 307–316.
- Klein, E.M., Karsten, J.L., 1995. Ocean-ridge basalts with convergent-margin geochemical affinities from the Chile Ridge. *Nature* 374, 52–57.
- Kogiso, T., Tatsumi, Y., Nakano, S., 1997. Trace element transport during dehydration processes in the subducted oceanic crust: 1. Experiments and implications for the origin of ocean island basalts. *Earth Planet. Sci. Lett.* 148, 193–205.
- Lee, C.-T.A., Luffi, P., Chin, E.J., Bouchet, R., Dasgupta, R., Morton, D.M., Le Roux, V., Yin, Q.-Z., Jin, D., 2012. Copper systematics in arc magmas and implications for crust–mantle differentiation. *Science* 336, 64–68.
- Li, W.Q., Jackson, S.E., Pearson, N.J., Alard, O., Chappell, B.W., 2009. The Cu isotopic signature of granites from the Lachlan fold belt, SE Australia. *Chem. Geol.* 258, 38–49.
- Li, W.Q., Jackson, S.E., Pearson, N.J., Graham, S., 2010. Copper isotopic zonation in the Northparkes porphyry Cu–Au deposit, SE Australia. *Geochim. Cosmochim. Acta* 74, 4078–4096.
- Li, D., Liu, S.-A., Li, S., 2015. Copper isotope fractionation during adsorption onto kaolinite: experimental approach and applications. *Chem. Geol.* 396, 74–82.
- Liu, J., Rudnick, R.L., Walker, R.J., Gao, S., Wu, F.Y., Piccoli, P.M., 2010. Processes controlling highly siderophile element fractionations in xenolithic peridotites and their influence on Os isotopes. *Earth Planet. Sci. Lett.* 297, 287–297.
- Liu, J.-G., Rudnick, R.L., Walker, R.J., Gao, S., Wu, F.-Y., Piccoli, P.M., Yuan, H., Xu, W.-L., Xu, Y.-G., 2011. Mapping lithospheric boundaries using Os isotopes of mantle xenoliths: an example from the North China Craton. *Geochim. Cosmochim. Acta* 75, 3881–3902.
- Liu, S.-A., Li, D.-D., Li, S.-G., Teng, F.-Z., Ke, S., He, Y.-S., Lu, Y.-H., 2014a. High-precision copper and iron isotope analysis of igneous rock standards by MC-ICP-MS. *J. Anal. At. Spectrom.* 29, 122–133.
- Liu, S.-A., Teng, F.-Z., Li, S., Wei, G.-J., Ma, J.-L., Li, D., 2014b. Copper and iron isotope fractionation during weathering and pedogenesis: insights from saprolite profiles. *Geochim. Cosmochim. Acta* 146, 59–75.
- Luck, J.M., Othman, D.B., Barrat, J.A., Albarède, F., 2003. Coupled ^{63}Cu and ^{16}O excesses in chondrites. *Geochim. Cosmochim. Acta* 67, 143–151.
- Maréchal, C.N., Télouk, P., Albarède, F., 1999. Precise analysis of copper and zinc isotopic compositions by plasma-source mass spectrometry. *Chem. Geol.* 156, 251–273.
- Mathur, R., Titley, S., Barra, F., Brantley, S., Wilson, M., Phillips, A., Munizaga, F., Maksae, V., Vervoort, J., Hart, G., 2009. Exploration potential of Cu isotope fractionation in porphyry copper deposits. *J. Geochem. Explor.* 102, 1–6.
- Mathur, R., Jin, L., Prush, V., Paul, J., Ebersole, C., Fornadel, A., Williams, J.Z., Brantley, S., 2012. Cu isotopes and concentrations during weathering of black shale of the Marcellus formation, Huntingdon County, Pennsylvania (USA). *Chem. Geol.* 304–305, 175–184.
- Mckenzie, D., O'niions, R.K., 1995. The source regions of oceanic island basalts. *J. Petrol.* 36, 133–159.

- Moeller, K., Schoenberg, R., Pedersen, R.-B., Weiss, D., Dong, S., 2012. Calibration of the new certified reference materials ERM-AE633 and ERM-AE647 for copper and IRMM-3702 for zinc isotope amount ratio determinations. *Geostand. Geoanal. Res.* 36, 177–199.
- Mungall, J.E., 2002. Roasting the mantle: slab melting and the genesis of major Au and Au-rich Cu deposits. *Geology* 30, 915–918.
- Münker, C., Wörner, G., Yogodzinski, G., Churikova, T., 2004. Behaviour of high field strength elements in subduction zones: constraints from Kamchatka–Aleutian arc lavas. *Earth Planet. Sci. Lett.* 224, 275–293.
- Olker, B., Altherr, R., Paquin, J., 2003. Fast exhumation of the ultrahigh-pressure Alpe Arami garnet peridotite (Central Alps, Switzerland): constraints from geospeedometry and thermal modelling. *J. Metamorph. Geol.* 21, 395–402.
- Plank, T., Langmuir, C.H., 1998. The chemical composition of subducting sediment and its consequences for the crust and mantle. *Chem. Geol.* 145, 325–394.
- Reisberg, L., Zhi, X., Lorand, J.-P., Wagner, C., Peng, Z., Zimmermann, C., 2005. Re–Os and S systematics of spinel peridotite xenoliths from east central China: evidence for contrasting effects of melt percolation. *Earth Planet. Sci. Lett.* 239, 286–308.
- Ripley, E.M., Brophy, J.G., Li, C., 2002. Copper solubility in a basaltic melt and sulfide liquid/silicate melt partition coefficients of Cu and Fe. *Geochim. Cosmochim. Acta* 66, 2791–2800.
- Rudnick, R.L., Gao, S., Ling, W.L., Liu, Y.S., McDonough, W.F., 2004. Petrology and geochemistry of spinel peridotite xenoliths from Hannuoba and Qixia, North China Craton. *Lithos* 77, 609–637.
- Savage, P., Chen, H., Shofner, G., Badro, J., Moynier, F., 2013. The copper isotope composition of bulk Earth: a new paradox. *Goldschmidt abstracts*, P2142.
- Savage, P., Jason, H., Frederic, M., 2014. Copper isotope heterogeneity in the lithospheric mantle. *Goldschmidt abstracts*, P2192.
- Savage, P., Moynier, F., Cheng, H., Shofner, G., Siebert, J., Badro, J., Puchtel, I.S., 2015. Copper isotope evidence for large-scale sulphide fractionation during Earth's differentiation. *Geochem. Perspect. Lett.* 1, 53–64.
- Sossi, P.A., Halverson, G.P., Nebel, O., Eggins, S.M., 2015. Combined separation of Cu, Fe and Zn from rock matrices and improved analytical protocols for stable isotope determination. *Geostand. Geoanal. Res.* 39, 129–149.
- Sun, S., McDonough, W., 1989. Chemical and isotopic systematics of oceanic basalts: implications for mantle composition and processes. *Geol. Soc. (Lond.) Spec. Publ.* 42, 313.
- Tang, Y.-J., Zhang, H.-F., Ying, J.-F., 2006. Asthenosphere–lithospheric mantle interaction in an extensional regime: implication from the geochemistry of Cenozoic basalts from Taihang Mountains, North China Craton. *Chem. Geol.* 233, 309–327.
- Vance, D., Archer, C., Bermin, J., Perkins, J., Statham, P.J., Lohan, M.C., Ellwood, M.J., Mills, R.A., 2008. The copper isotope geochemistry of rivers and the oceans. *Earth Planet. Sci. Lett.* 274, 204–213.
- Wegner, W., Wörner, G., Harmon, R., Jicha, B., 2011. Magmatic history and character of the Central American Land Bridge region since Cretaceous time. *Geol. Soc. Am. Bull.* 123, 703–724.
- Weyer, S., Ionov, D.A., 2007. Partial melting and melt percolation in the mantle: the message from Fe isotopes. *Earth Planet. Sci. Lett.* 259, 119–133.
- Yang, W., Li, S.G., 2008. Geochronology and geochemistry of the Mesozoic volcanic rocks in Western Liaoning: implications for lithospheric thinning of the North China Craton. *Lithos* 102, 88–117.
- Yogodzinski, G., Lees, J., Churikova, T., Dorendorf, F., Woerner, G., Volynets, O., 2001. Geochemical evidence for the melting of subducting oceanic lithosphere at plate edges. *Nature* 409, 500–504.
- Zhang, R.Y., Liou, J.G., Yang, J.S., Yui, T.F., 2000. Petrochemical constraints for dual origin of garnet peridotites from the Dabie–Sulu UHP terrane, eastern-central China. *J. Metamorph. Geol.* 18, 149–166.
- Zheng, J.P., Zhang, R.Y., Griffin, W.L., Liou, J.G., O'reilly, S.Y., 2005. Heterogeneous and metasomatized mantle recorded by trace elements in minerals of the Donghai garnet peridotites, Sulu UHP terrane, China. *Chem. Geol.* 221, 243–259.
- Zheng, J.P., Sun, M., Griffin, W.L., Zhou, M.F., Zhao, G.C., Robinson, P., Tang, H.Y., Zhang, Z.H., 2008. Age and geochemistry of contrasting peridotite types in the Dabie UHP belt, eastern China: petrogenetic and geodynamic implications. *Chem. Geol.* 247, 282–304.
- Zhu, X.K., O'Nions, R.K., Guo, Y., Belshaw, N.S., Rickard, D., 2000. Determination of natural Cu-isotope variation by plasma-source mass spectrometry: implications for use as geochemical tracers. *Chem. Geol.* 163, 139–149.